

Performance Characteristics and Thermodynamic Investigations on Single-Stage Thermoelectric Generator and Heat Pump Systems

Rajesh Arora^{1*} and Ranjana Arora²

¹*Department of Mechanical Engineering, Amity University Haryana, Gurgaon-122413, India*

²*Renewable Energy Department, Amity University Haryana, Gurgaon-122413, India*

ABSTRACT

The thermodynamic analysis of thermoelectric devices (TEs) discards the impact caused by heat leak between source and sink. It could lead towards the partial/incomplete modelling of TEs along with some analytical gaps in their performance evaluation. Conversely, appropriate agreement among different design constraints of TEs is a must to upgrade their operating characteristics. In view of this, the modelling of multi-element single-stage thermoelectric generator (TEG) and thermoelectric heat pump (TEHP) is carried out in matrix laboratory (MATLAB 9.2). The irreversibilities caused by heat leak between the source/sink along with Fourier/Joule effects are considered for the modelling and analysis. The power output/thermal efficiency and heating capacity/coefficient of performance (COP) of TEs are analytically derived and optimized on the basis of finite time thermodynamic principles. The predetermined thermoelectric couples are chosen to maximize the heating capacity/COP in proposed configurations. Moreover, the influence of design variables viz electrical current, thermoelectric couples on system throughput is analyzed and presented. The effects of geometrical parameters viz length and area of individual modules on the performance of TEG and TEHP are also discussed.

Keywords: Finite time thermodynamic, thermoelectric generators, thermoelectric heat pumps, (FTT), thermodynamic optimization

ARTICLE INFO

Article history:

Received: 07 February 2018

Accepted: 28 May 2018

Published: 24 October 2018

E-mail addresses:

rajesharora1219@rediffmail.com (Rajesh Arora)

ranjana1219@rediffmail.com (Ranjana Arora)

* Corresponding author

INTRODUCTION

In today's era, the rapid rise in energy demand has led researchers/scientists to search for new resources of energy. As the conventional energy resources are coming to an end, innovative/smart energy conversion technologies are gaining wide

attraction globally. Due to non-moving parts, low maintenance requirements, low/zero noise operation, compact configuration and small volume occupancy, these are getting very popular amongst various commercial applications. The thermoelectric devices viz. thermoelectric generators and heat pumps are direct thermal to electricity conversion devices requiring low maintenance, capable to operate in modular form and have possibility to utilize heat from sources over a wide range of temperature (Angrist, 1994; Disalvo, 1999; Goldsmith, 1964; Rowe, 2005). These devices consist of a semiconductor thermocouple having two junctions. When these two junctions, named as hot junction and cold junction are maintained at different temperatures, the voltage is generated in the order of microvolts/Kelvin. This is known as Seebeck effect. The reverse effect in which a junction can be heated or cooled with the passage of current through it, is known as Peltier effect. Several thermocouples are joined in electrically series configuration to have desired voltage output (Chen & Wu, 2000; Min et al., 2003; Riffat & Ma, 2003; Xuan et al., 2002). Thermoelectric devices are coupled with the source/sink and according to classical thermodynamics, it takes infinite time for heat transfer between system and coupled thermal reservoirs. This is not desirable from practical point of view. The finite time heat transfers are the need of practical thermoelectric devices to obtain finite output power/thermal efficiency, heating capacity/coefficient of performance (Andresen, 1983). It is observed that classical thermodynamic does not provide the comprehensive picture of equilibrium states/reversible processes. On the other hand, finite time thermodynamic (FTT) provides an extension to conventional thermodynamic theory as it accounts for finite time consumption of heat transfer between system and coupled thermal reservoirs. Finite time thermodynamic approach takes into account both external and internal irreversibilities of the system. In thermoelectric devices, internal irreversibility is because of Joule/conduction heat loss while external irreversibility is because of finite rate heat transfers between heat reservoirs/system (Chen et al., 1994). In the present literature, several investigations are carried out on thermodynamic optimization and analysis of thermoelectric generators/heat pumps with conventional/non-equilibrium thermodynamics. Chen et al. (2005a) enunciated optimization of series mode operated multi-stage TEG with respect to different designing operators. Afterwards, they investigated the characteristics of thermoelectric refrigerator (Chen et al., 2005b). Later, Chen et al. (2008) optimized the throughput of 2-stage heat pumps in electrically series mode with internal/external irreversibilities employing finite time thermodynamic (FTT) principles. David et al. (2012) investigated thermodynamic studies and optimizations of TEHP in view of different design/operating variables and designed a heat exchanger for a system. Afterwards, an experimental model of TEGs had been tested in order to characterize the different performance parameters (Chen et al., 2012; Zhu et al., 2011). A comprehensive comparison of single/two-stage series connected TEGs operating with an automobile exhaust was demonstrated by Sun et al. (2014). They observed that two-stage system can

yield better output in case of high source-side temperature. Riffat et al. (2004) developed the strategy to optimize thermoelectric modules for space conditioning applications where as the optimum design of the modules for space heating applications in the buildings was presented by Kim et al. (2014). Kaushik et al. (2015) analyzed single-stage thermoelectric heat pumps (TEHP) in view of energy/exergy concepts. They noticed that the effects of internal irreversibility were more in comparison with external irreversibility. Hans et al. (2015) enunciated an optimization study for series/ parallel modes operated TEGs, with respect to various design variables for obtaining maximum output power and first law efficiency. Later, they carried out the comparative performance optimization of 2-stage thermoelectric heat pumps in three different modes (Hans et al., 2016). Further, Kumar and Pandey (2017) calculated the efficiency of a TEG in order to study the impacts of different thermoelectric materials.

In the present literature, a few thermodynamic investigations and optimization studies are available on multi-element single-stage thermoelectric generators and heat pumps (Hans et al. 2015; Nami et al. 2017; Tan et al. 2017). Moreover, the influence of heat leak between the source and sink has not been considered which leads to incomplete modelling of the system. Additionally, there is a need of analyzing the effects of geometric variables and temperature dependent physical properties on performance parameters and optimal designing of thermoelectric devices. In this context, the thermodynamic models of multi-element irreversible TEG and TEHP systems taking into account both internal and external effects, with and without heat leak between source and sink are developed in MATLAB. The performance analysis of above mentioned devices is done on the basis of Newton's law of heat transfer and finite time thermodynamic principles. A comparative study of multi-element irreversible TEG and TEHP based on finite time thermodynamic modeling is carried out considering internal/ external effects. A formulation of performance parameters of thermoelectric devices with respect to electric current, thermoelectric couples, temperature of hot/cold side and thermal conductances of hot/cold side is presented. The internal irreversibilities are caused by Joule/conduction heat losses while, external irreversibilities are because of finite heat transfers between reservoir and devices. The impacts of design factors on output power/thermal efficiency and heating capacity/ coefficient of performance (COP) are analyzed and outcomes are presented graphically. The effects of geometric parameters viz. length and area of thermoelectric elements have been investigated on performance aspects of above mentioned systems. The geometry of the thermoelectric element is directly linked to thermoelectric material and cost of manufacturing. The major outcomes of this study are the comparative investigations along with novel analytical and parametric analysis of multi-element thermoelectric systems with and without heat leak considerations.

Finite-Time Thermodynamic Modeling of Thermoelectric Devices

Thermodynamic modeling of multi-element single-stage thermoelectric generator (TEG) and thermoelectric heat pumps (TEHP) with both external/internal irreversibilities is done through finite-time thermodynamic principles. The thermodynamic modeling of the proposed TEs has been carried out based on the following assumptions.

- Steady-state one-dimensional heat flow has been considered.
- The exoreversible configurations with negligible contact/interconnection resistances are considered.
- The Thomson effect in thermoelectric elements is not taken into account.
- Convection and radiation losses in thermoelectric elements are not considered.
- The material used for TECs is assumed to be Bismuth Telluride (Bi_2Te_3).

The following temperature reliant properties of the thermoelectric materials, as given by Xuan et al. (2002) are used in the present study.

$$\alpha = [\alpha_p - (-\alpha_n)] = 2 \times (22224.0 + 930.6T_{av} - 0.9905T_{av}^2) \times 10^{-9} V / K \quad (1)$$

$$\rho_n = \rho_p = (5112.0 + 163.4T_{av} + 0.6279T_{av}^2) \times 10^{-10} \Omega / m \quad (2)$$

$$k_n = k_p = (62605.0 - 277.7T_{av} + 0.413T_{av}^2) \times 10^{-4} W / mK \quad (3)$$

$$\tau = [\tau_p - (-\tau_n)] = 2 \times (930.6T_{av} - 1.981T_{av}^2) \times 10^{-9} V / K \quad (4)$$

$$T_{av} = \left(\frac{T_h + T_c}{2} \right) \quad (5)$$

$$R = \left(\frac{\rho_p L_p}{A_p} + \frac{\rho_n L_n}{A_n} \right) \quad (6)$$

$$K = \left(\frac{k_p A_p}{L_p} + \frac{k_n A_n}{L_n} \right) \quad (7)$$

Thermodynamic Modeling of Single-Stage Thermoelectric Generator (TEG)

The TEG model with P/N type semiconductor legs is illustrated in Figure 1(a). The thermoelectric couples are arranged in electrical series and thermally parallel configurations in pursuance of generating a considerable voltage output from the system. The generalized TEG model revealing the heat flow and generating the electrical output is presented in Figure 1(b). In corresponding figures, T_H and T_h signifies the input source/hot junction

temperatures whereas the T_L and T_c are the heat sink and cold junction ones. Larger the differential temperature amongst the two junctions, more is the potential difference generated at external resistance R_L .

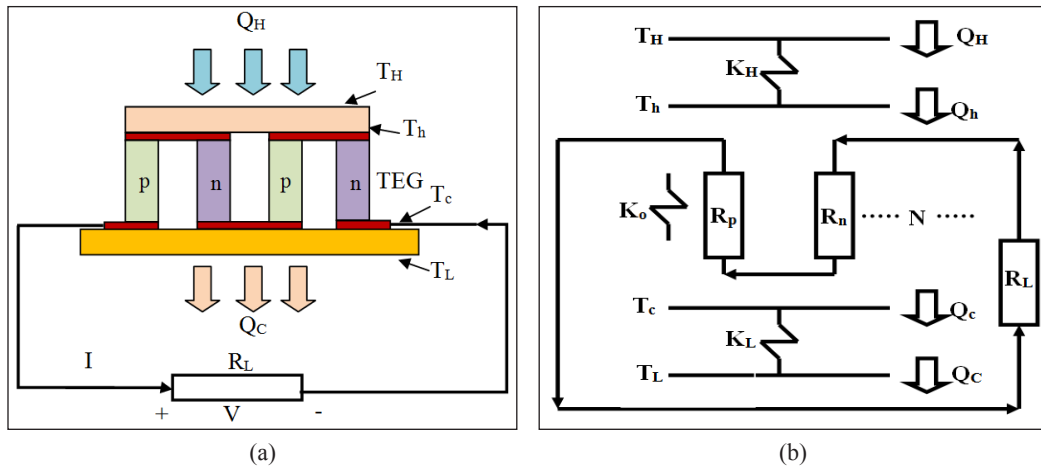


Figure 1. (a) Single-stage TEG; and (b) Generalized FTT model of TEG

The energy equations for P-type semiconductor legs can be written as

$$Q_{Kin} - Q_{Kout} + Q_J = 0 \tag{8}$$

where, Q_{Kin} and Q_{Kout} are the heat input/output of the thermoelectric elements by conduction and Q_J is the Joule heat generated in the element. Equation 8 can be rewritten as

$$\frac{d}{dx}(T_p + dT_p)k_p A_p - \frac{dT_p}{dx}k_p A_p + (J_p)^2 \frac{A_p L_p dx}{\sigma_p L_p} = 0 \tag{9}$$

Similarly, the equation for N-type semiconductor leg can be stated as

$$\frac{d}{dx}(T_n + dT_n)k_n A_n - \frac{dT_n}{dx}k_n A_n + (J_n)^2 \frac{A_n L_n dx}{\sigma_n L_n} = 0 \tag{10}$$

Boundary conditions for P/N types semiconductor leg can be given as

$$T_p(0) = T_n(0) = T_c \tag{11}$$

$$T_p(L_p) = T_n(L_p) = T_h \tag{12}$$

The temperature dependent thermoelectric properties k_p , σ_p are the functions of T_p and k_n , σ_n are the functions of T_n . Putting the boundary conditions to Equations (9) and (10) and substituting k , σ by their mean values \bar{k} and $\bar{\sigma}$, differential equations can be given as

$$\bar{k}_p A_p \frac{d^2 T_p}{dx^2} + \frac{I^2}{\sigma_p A_p} = 0 \tag{13}$$

$$\bar{k}_N A_N \frac{d^2 T_N}{dx^2} + \frac{I^2}{\sigma_N A_N} = 0 \quad (14)$$

The total heat flows via the hot-side/cold-side junctions are

$$Q_h = N \left((\alpha_{Ph} - \alpha_{Nh}) T_h I + k_P \Big|_{x=L_P} A_P \frac{dT_P}{dx} \Big|_{x=L_P} + k_N \Big|_{x=L_N} A_N \frac{dT_N}{dx} \Big|_{x=L_N} \right) \quad (15)$$

$$Q_c = N \left((\alpha_{Pc} - \alpha_{Nc}) T_c I + k_P \Big|_{x=0} A_P \frac{dT_P}{dx} \Big|_{x=0} + k_N \Big|_{x=0} A_N \frac{dT_N}{dx} \Big|_{x=0} \right) \quad (16)$$

The rate of heat flows from heat source/sink are given as

$$Q_H = K_H (T_H - T_h) \quad (17)$$

$$Q_C = K_L (T_c - T_L) \quad (18)$$

The heat flows from hot/cold junctions are given as

$$Q_h = N[\alpha_h I T_h + k(T_h - T_c) - 0.5 I^2 R] \quad (19)$$

$$Q_c = N[\alpha_c I T_c + k(T_h - T_c) + 0.5 I^2 R] \quad (20)$$

Where,

$$\alpha_h = \alpha_{hp} - \alpha_{hm} \text{ and } \alpha_c = \alpha_{ch} - \alpha_{cp}$$

According to heat flow balance, one can have following condition as

$$Q_H = Q_h \quad (21)$$

$$Q_C = Q_c \quad (22)$$

The output is given by

$$P = Q_h - Q_c \quad (23)$$

By putting the values of Q_h and Q_c in Eq. (23) from Equations (19) and (20)

$$P = NI(\alpha_h T_h - \alpha_c T_c - IR) \quad (24)$$

The efficiency is given by

$$\eta = \frac{P}{Q_h} = \frac{NI[\alpha_h T_h - \alpha_c T_c - IR]}{N[\alpha_h I T_h + k(T_h - T_c) - 0.5 I^2 R]} \quad (25)$$

Putting, $\alpha_h = \alpha_c = \alpha$

From above Equations, one can get T_h and T_c as

$$T_h = \frac{0.5N^2\alpha RI^3 + (-N^2Rk - 0.5NRK_L)I^2 + N\alpha K_H T_H I - NK(K_H T_H + K_L T_L) - K_L K_H T_H}{N^2\alpha^2 I^2 + N\alpha I(K_H - K_L) - NK(K_H + K_L) - K_L K_H} \quad (26)$$

$$T_c = \frac{0.5N^2\alpha RI^3 + (N^2Rk + 0.5NRK_H)I^2 + N\alpha K_L T_L I + NK(K_H T_H + K_L T_L) + K_L K_H T_L}{-N^2\alpha^2 I^2 + N\alpha I(K_L - K_H) + NK(K_H + K_L) + K_L K_H} \quad (27)$$

TEG Model with Heat Leak between Source and Sink

The heat flows from hot/cold junctions due to small heat leak is given as

$$Q'_c = N[\alpha_c I T_c + k(T_h - T_c) + 0.5I^2 R + K_0(T_c - T_L)] \quad (28)$$

$$Q'_h = N[\alpha_h I T_h + k(T_h - T_c) + 0.5I^2 R + K_0(T_c - T_L)] \quad (29)$$

The output is given as

$$P = Q'_h - Q'_c \quad (30)$$

The efficiency in this case can be given as

$$\eta = \frac{P}{Q'_h} = \frac{NI[\alpha_h T_h - \alpha_c T_c - IR]}{N[\alpha_h I T_h + k(T_h - T_c) - 0.5I^2 R + K_0(T_h - T_L)]} \quad (31)$$

The values of various parameters used in FTT modeling of multi-element TEG is given in Table 1.

Table 1
Value (s) of various parameters

Parameters	Values
R	$2.885 \times 10^{-3} \Omega$
K	0.02772 W/K
α	$425 \times 10^{-6} \text{ V/K}$
T_H	400 K
T_L	300 K
N	127
$K_H=K_L$	10W/K

Source: (Chen et al., 2005)

Thermodynamic Modeling of Single-Stage Thermoelectric Heat Pump (TEHP)

The TEHP model with P/N type semiconductor legs is illustrated in Figure 2(a). The thermoelectric couples are arranged in electrical series and thermally parallel configurations. The generalized TEHP model revealing the heat flow and with the electrical input is presented in Figure 2(b). In corresponding figures, T_H and T_h signifies the input source/hot junction temperatures whereas the T_L and T_c are the heat sink and cold junction ones.

When electrical current, 'I' flows through TEHP, heat flows $NaIT_c$ and $NaIT_h$ are captivated from the surroundings and rejected to the space to be heated. The heat source is maintained at low temperature whereas the sink i.e., heated space is maintained at high temperature.

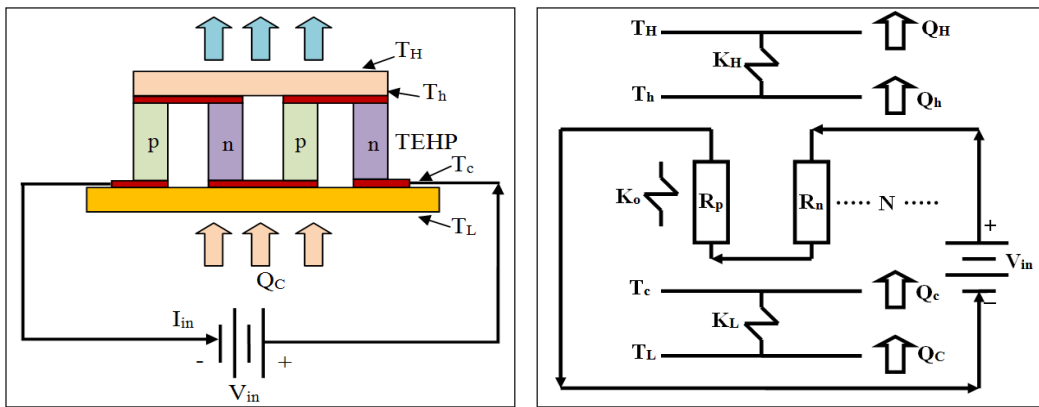


Figure 2. (a) Single stage TEHP; and (b) Generalized FTT model of TEHP

The energy equations of P-type semiconductors are given as

$$Q_{Kin} - Q_{Kout} + Q_J = 0 \tag{32}$$

where, Q_{Kin} and Q_{Kout} are the heat input/output of the thermoelectric element by conduction and Q_J is the Joule heat generated in the element. Eq. 32 can be rewritten as

$$\frac{d}{dx}(T_p + dT_p)k_p A_p - \frac{dT_p}{dx}k_p A_p + (J_p)^2 \frac{A_p L_p dx}{\sigma_p L_p} = 0 \tag{33}$$

Similarly, the equation for N-type semiconductor leg can be written as

$$\frac{d}{dx}(T_n + dT_n)k_n A_n - \frac{dT_n}{dx}k_n A_n + (J_n)^2 \frac{A_n L_n dx}{\sigma_n L_n} = 0 \tag{34}$$

Boundary conditions for P and N type semiconductor legs can be given as

$$T_p(0) = T_n(0) = T_c \tag{35}$$

$$T_p(L_p) = T_N(L_p) = T_h \quad (36)$$

The temperature dependent thermoelectric properties k_p , σ_p are the functions of T_p and k_N , σ_N are the functions of T_N . Putting the boundary conditions to Equations (33) and (34) and substituting k , σ by their mean values \bar{k} and $\bar{\sigma}$, differential equations can be given as

$$\bar{k}_N A_N \frac{d^2 T_N}{dx^2} + \frac{I^2}{\bar{\sigma}_N A_N} = 0 \quad (37)$$

$$\bar{k}_N A_N \frac{d^2 T_N}{dx^2} + \frac{I^2}{\bar{\sigma}_N A_N} = 0 \quad (38)$$

The total heat flows via the hot-side/cold-side junctions are

$$Q_h = N \left((\alpha_{p_h} - \alpha_{n_h}) T_h I - k_p \Big|_{x=L_p} A_p \frac{dT_p}{dx} \Big|_{x=L_p} - k_N \Big|_{x=L_N} A_N \frac{dT_N}{dx} \Big|_{x=L_N} \right) \quad (39)$$

$$Q_c = N \left((\alpha_{p_c} - \alpha_{n_c}) T_c I - k_p \Big|_{x=0} A_p \frac{dT_p}{dx} \Big|_{x=0} - k_N \Big|_{x=0} A_N \frac{dT_N}{dx} \Big|_{x=0} \right) \quad (40)$$

The rate of heat flows from heat source/sink are given as

$$Q_H = K_H (T_h - T_H) \quad (41)$$

$$Q_C = K_L (T_L - T_c) \quad (42)$$

The rate of heat flows from hot/cold junctions are given as

$$Q_h = N[\alpha_h I T_h - k(T_h - T_c) + 0.5 I^2 R] \quad (43)$$

$$Q_c = N[\alpha_c I T_c - k(T_h - T_c) - 0.5 I^2 R] \quad (44)$$

Putting,

$$\alpha_h = \alpha_c = \alpha$$

According to heat flow balance, one can have following condition as

$$Q_H = Q_h \quad (45)$$

$$Q_C = Q_c \quad (46)$$

The heating power is given by

$$P = Q_h - Q_c \quad (47)$$

The COP of TEHP can be calculated as

$$COP = \frac{Q_h}{Q_h - Q_c} \quad (48)$$

From Eqs. (45) and (46), one can get T_h and T_c as

$$T_h = \frac{0.5N^2\alpha RI^3 + (N^2Rk + 0.5NRK_L)I^2 + N\alpha K_H T_H I + NK(K_H T_H + K_L T_L) + K_L K_H T_H}{-N^2\alpha^2 I^2 + N\alpha I(K_H - K_L) + NK(K_H + K_L) + K_L K_H} \quad (49)$$

$$T_c = \frac{0.5N^2\alpha RI^3 + (-N^2Rk - 0.5NRK_L)I^2 + N\alpha K_H T_H I - NK(K_H T_H + K_L T_L) - K_L K_H T_H}{N^2\alpha^2 I^2 + N\alpha I(K_L - K_H) - NK(K_H + K_L) - K_L K_H} \quad (50)$$

TEHP Model with Heat Leak between Source and Sink

The heat flows from hot/cold junctions due to small heat leak is given as

$$Q'_h = N[\alpha_h I T_h + k(T_h - T_c) - 0.5I^2 R - K_0(T_H - T_h)] \quad (51)$$

$$Q'_c = N[\alpha_c I T_c + k(T_h - T_c) + 0.5I^2 R - K_0(T_c - T_L)] \quad (52)$$

The heating power is given as

$$P = Q'_h - Q'_c \quad (53)$$

The COP of TEHP with heat leak

$$COP = \frac{Q'_h}{Q'_h - Q'_c} \quad (54)$$

The values of various parameter used in FTT modeling of multi-element TEHP system is given in Table 2.

Table 2
Value (s) of various parameters

Parameters	Values
R	$2.885 \times 10^{-3} \Omega$
K	0.02772 W/K
α	$425 \times 10^{-6} \text{ V/K}$
T_H	300 K
T_L	250 K
N	127
$K_H=K_L$	100 W/K

Source: (Chen et al., 2008)

DISCUSSION

Figure 3 shows the variations of output power (P) with electric current (I) for various values of sink temperature (T_L), assuming a fixed source temperatures (T_H) of multi-element TEG. The output power is a parabolic function of "I" and its peak value decreases as T_L increases. For a fixed value of source temperature, as T_L increases the temperature differences (DTG) between the heat source/sink decreases and power output eventually falls down.

Likewise, the variation of output power (P) with electric current (I) for various values of source temperatures (T_H), assuming a fixed sink temperature (T_L) of TEG is demonstrated in Figure 3. The output power is a parabolic function of I and its maximum value increases with increase in the value of T_H . For a fixed value of sink temperature, as T_H increases the temperature differences (DTG) between heat source and sink increases and power output ultimately goes up.

Figure 5 and Figure 6 shows the parabolic variations of first law efficiency (η) with I for different values of T_H and T_L respectively. The thermal efficiency increases as T_H increases (for fixed value of T_L) and drops with increase in T_L (for fixed value of T_H). The reason behind this is, as the value of DTG increases in TEG system the first law efficiency goes up and vice versa.

The variation of P with I for different number of thermoelectric elements (N) is illustrated in Figure 7. The output power attains its peak at an optimum value of N, nearly 120. Number of thermoelectric elements affects power output of TEG system for optimal values.

The variations in P and η with I for different values of thermal conductance at hot and cold junction (K_H and K_L) are illustrated in Figure 8 and Figure 9. As the value of K_H and K_L increases, maximum values attained by P and η also go up. The power output and thermal efficiency first increases with current but afterwards it decreases due to dominating effect

of Joule internal irreversibility (I^2R). Therefore, one has to obtain the optimum current with respect to desirable power output and thermal efficiency of the system for given set of design variables.

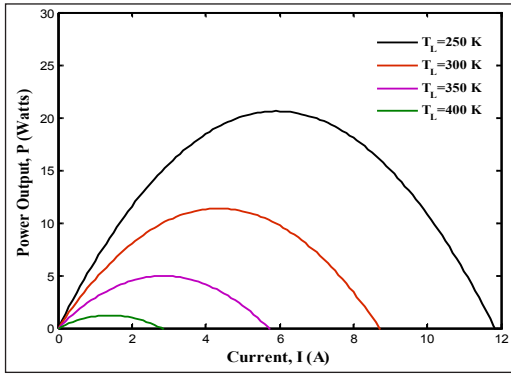


Figure 3. Power output vs 'I' with different values of ' T_L ' and fixed value of T_H for TEG

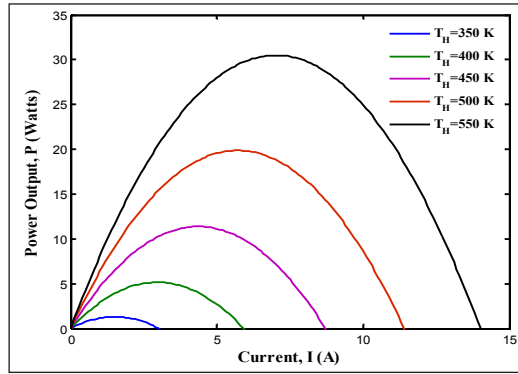


Figure 4. Power output vs 'I' with various values of ' T_H ' and fixed value of T_L for TEG

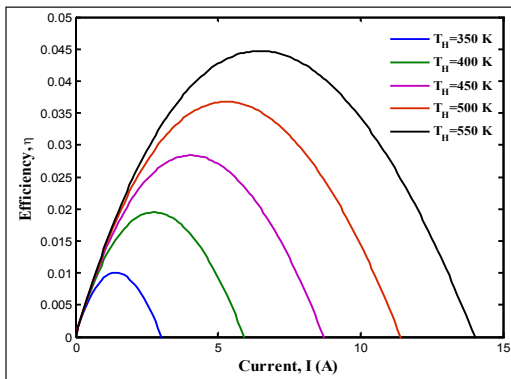


Figure 5. Thermal efficiency vs 'I' with various values of ' T_H ' and fixed value of T_L for TEG

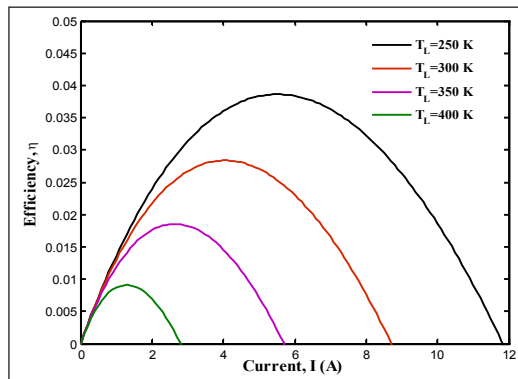


Figure 6. Thermal efficiency vs 'I' with different values of ' T_L ' and fixed value of T_H for TEG

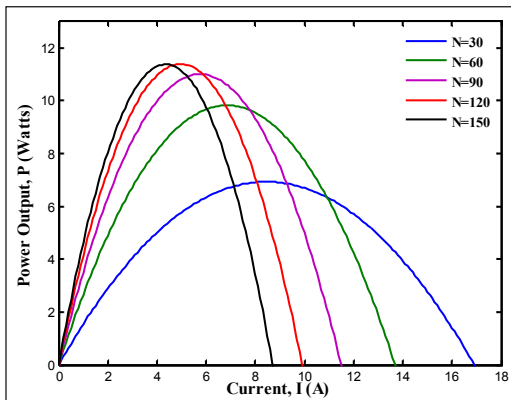


Figure 7. Power output vs 'I' with different values of number of thermoelectric elements for TEG

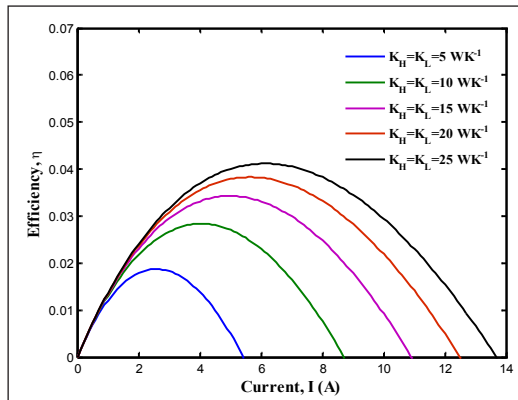


Figure 8. Thermal Efficiency vs 'I' with different values of K_H and K_L for TEG

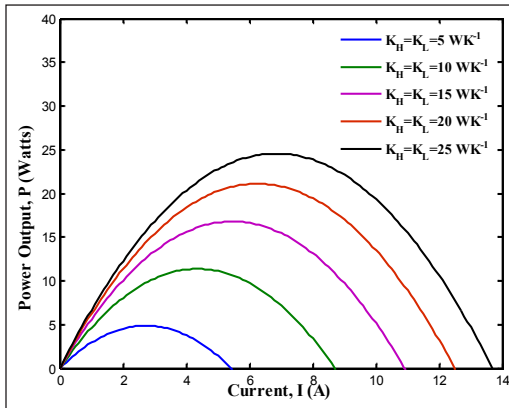


Figure 9. Power Output vs 'I' with different values of K_H and K_L for TEG

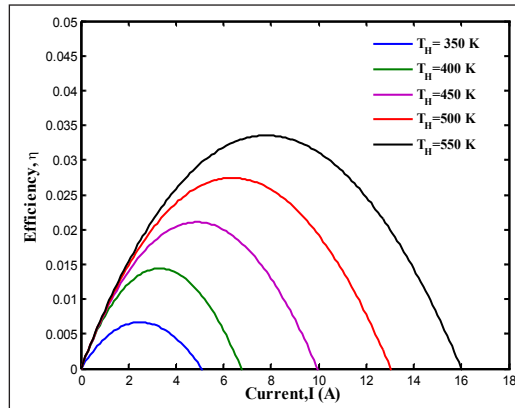


Figure 10. Thermal efficiency vs 'I' with different values of ' T_H ' and fixed ' T_L ' for TEG with heat leak between source and sink

Figure 10 to Figure 12 show the relationship of thermal efficiency with current for different values of T_H , T_L and thermal conductance (K_H and K_L) with addition of an external irreversibility K_0 in the system. This external irreversibility K_0 is because of heat leak between source/sink, due to which there is considerable drop in the value of maximum thermal efficiency attained by the device.

Figure 13 shows the variations of COP with electric current (I) for various values of sink temperature (T_L), assuming a fixed source temperatures (T_H) of multi-element TEHP. The COP initially increases up to a maximum limit and declines afterwards with working electrical current for all chosen values of T_L . The TEHP yields better COP as the value of sink temperature goes up because for fixed heat source temperature, as the temperature difference between source and sink (DTHP) decreases COP rises ultimately. Similarly, the variation of COP with electric current (I) for different values of source temperatures (T_H), assuming a fixed sink temperature (T_L) of TEHP is demonstrated in Figure 14 The TEHP yields reduced COP as the value of heat source temperature goes up because for fixed heat sink temperature, as DTHP increases COP drops considerably.

Figure 15 shows the variations of heating capacity (Q_h) with I for various values of T_H assuming a fixed heat sink temperature. The system attains a maximum heating capacity of nearly 115 Watts at $T_H=300K$ and minimum heating capacity of nearly 18Watts at $T_H=375K$. Hence, increase in source temperature inversely affects heating capacity of the system. The variation of COP and Q_h with I for different number of thermoelectric elements (N) is illustrated in Figure 16 and Figure 17. The heating capacity Q_h significantly goes up with number of thermoelectric elements. The maximum COP accomplished by multi-element TEHP system is higher for higher values of N .

The graphical relationships of COP and Q_h with I for different values of thermal conductance at hot and cold junction (K_H and K_L) are demonstrated in *Figure 18* and *Figure 19*. As the value of K_H and K_L increases, maximum value attained by COP decreases and Q_h increases ultimately.

Figure 20 and *Figure 21* show the relationship of Q_h with current for different values of N and thermal conductance (K_H and K_L) with addition of an external irreversibility K_0 in the system. This external irreversibility K_0 is because of this additional heat leak between source/sink, due to which there is considerable drop in the value of maximum heating capacity attained by the system, as we compare these values from *Figure 17* and *Figure 19*. Correspondingly, by comparing *Figures 22* to *23* and *Figures 16* to *18*, one can make out the fall in COP of TEHP due to heat leak between source and sink.

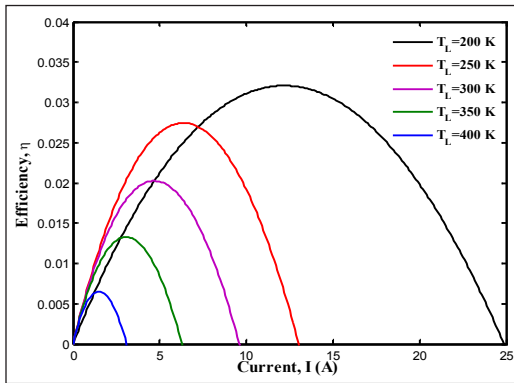


Figure 11. Thermal efficiency vs 'I' with different values of ' T_L ' and fixed ' T_H ' for TEG with heat leak between source and sink

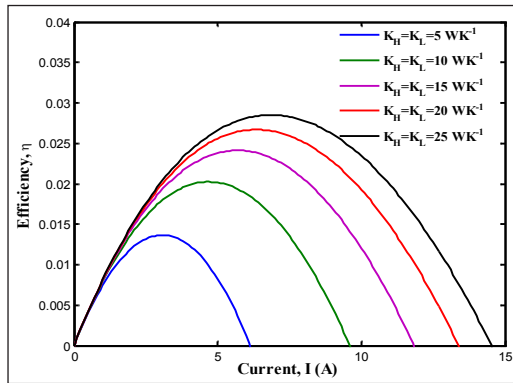


Figure 12. Thermal efficiency vs 'I' with different values of K_H and K_L for TEG with heat leak between source and sink

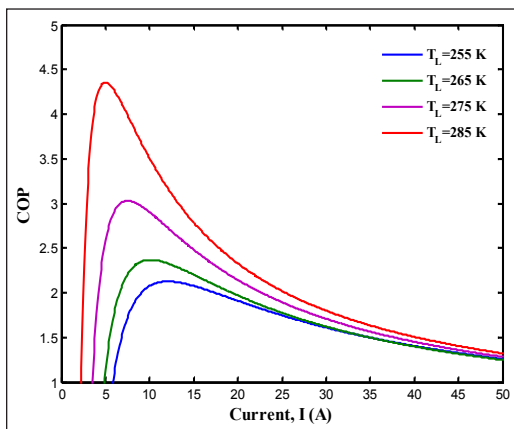


Figure 13. COP vs 'I' with different values of T_L and fixed value of T_H for TEHP

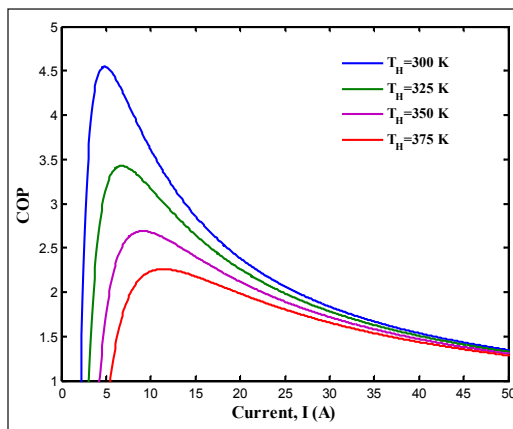


Figure 14. COP vs 'I' with different values of T_H and fixed value of T_L for TEHP

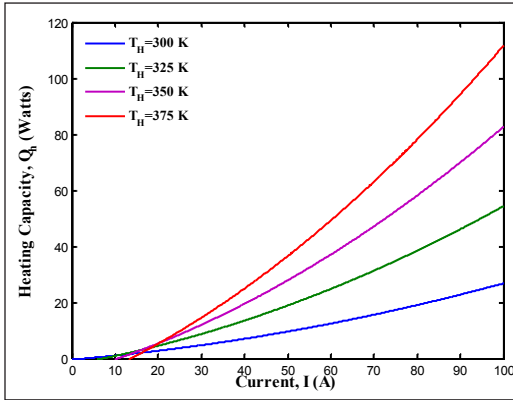


Figure 15. Heating capacity vs 'I' with different values of T_H and fixed value of T_L for TEHP

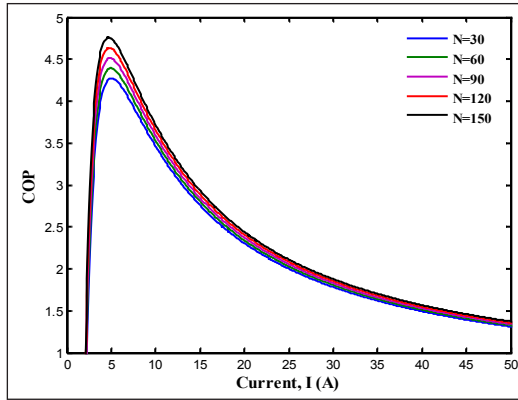


Figure 16. COP vs 'I' with different values of number of thermoelectric elements for TEHP

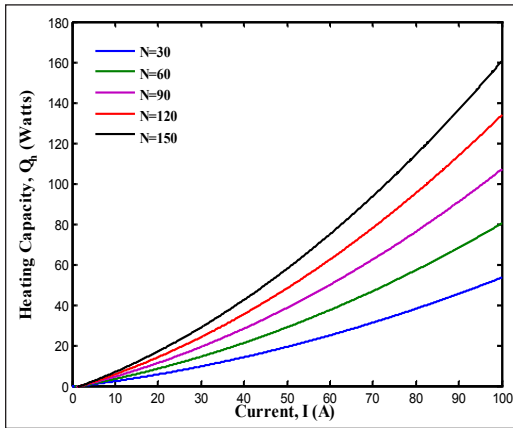


Figure 17. Heating capacity vs 'I' with different values of number of thermoelectric elements for TEHP

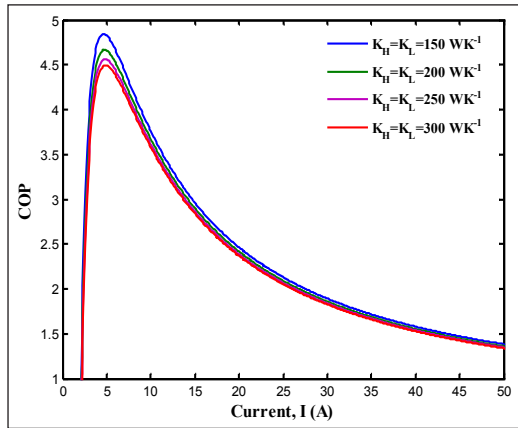


Figure 18. COP vs 'I' with different values of K_H and K_L for TEHP

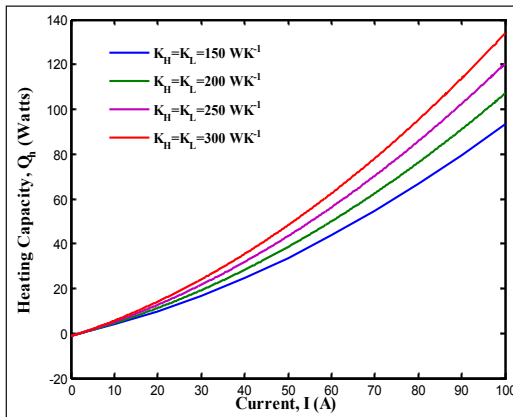


Figure 19. Heating capacity vs 'I' with different values of K_H and K_L for TEHP

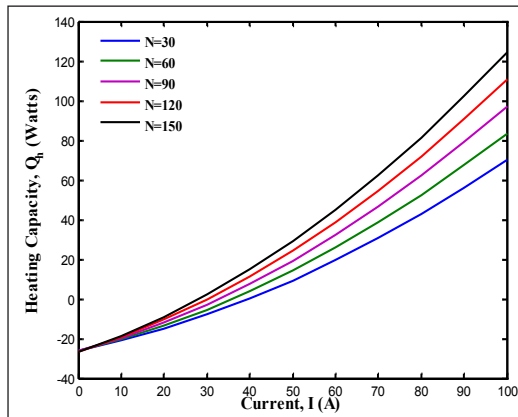


Figure 20. Heating capacity vs 'I' with different values of 'N' for TEHP with heat leak between source and sink

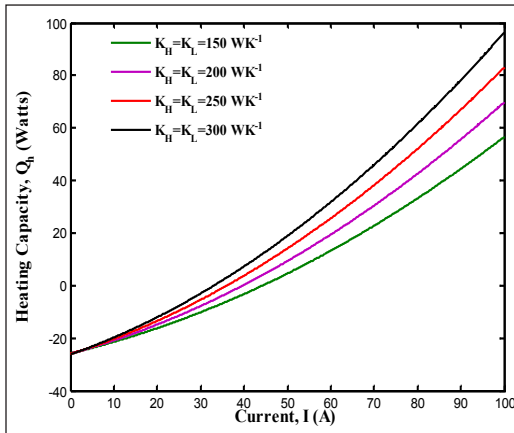


Figure 21. Heating capacity vs ‘I’ with different values of K_H and K_L for TEHP with heat leak between source and sink

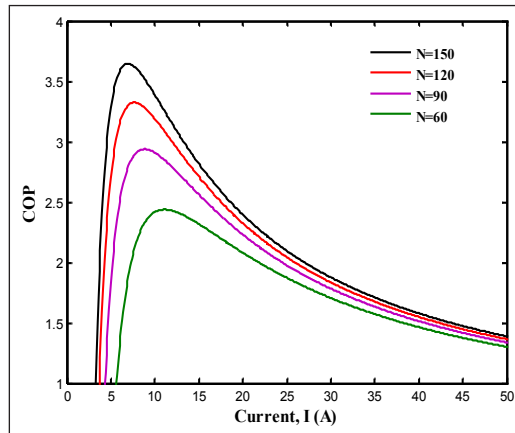


Figure 22. COP vs ‘I’ with different values of ‘N’ for TEHP with heat leak between source and sink

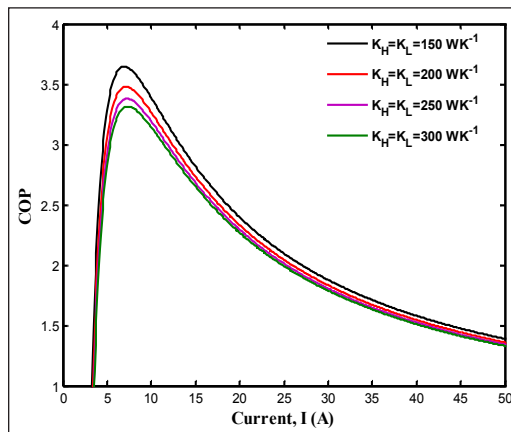


Figure 23. COP vs ‘I’ with different values of K_H and K_L for TEHP with heat leak between source and sink

Effect of Geometric Parameters on the Single-Stage TEG and the Systems

The power output/first law efficiency of TEG depends on the working electric current, I and for given design parameters, there exists optimal electric current related to which peak power and thermal efficiency can be obtained. Similarly, maximum COP and heating capacity can be obtained for optimal values of working electrical current. From the previous literature, it can be observed that geometry of thermoelectric elements can significantly affect the performance parameters viz. output power, first law efficiency, COP and heating capacity of thermoelectric devices. The geometric parameters comprises length and area of thermoelectric elements.

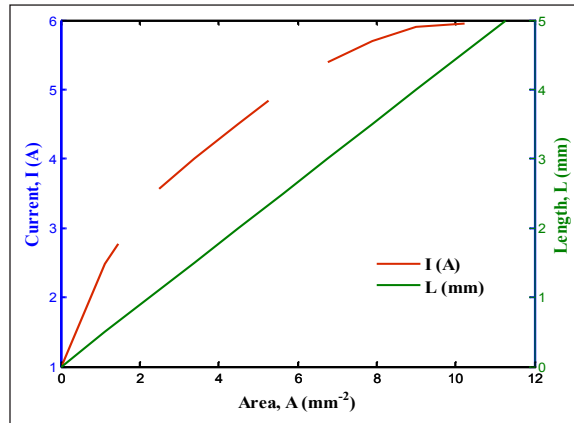


Figure 24. Variations of current and length with area of the thermoelectric element

Figure 24 shows the variations of electric current and length with area of thermoelectric couples. It is observed that length possess a linear relationship with the corresponding area of thermoelectric elements whereas the working electrical current initially increases with increase in area and stabilizes afterwards. It is clearly shown that the working electrical current is influenced by the geometric parameters of thermoelectric elements. Therefore, variations in length and area can considerably vary the required performance characteristics of thermoelectric devices. These geometric parameters are associated with the economical aspects of designing and hence, their optimum value should be chosen by appropriate numerical computations.

Figure 25 demonstrates the variations of power output with area for different values source side temperature T_H for an irreversible single stage TEG system. For numerical computation the values of other parameters are chosen as $T_L=300\text{K}$, $K_H=K_L=10\text{W/K}$, $L=0.5\text{mm}$, $I=5\text{A}$ and $N=127$. For a fixed value of sink side temperature T_L , as T_H goes up the value of $\Delta T(T_H-T_L)$ increases and as a result the corresponding power output enhances. Initially the power output sharply rises with area 'A' but subsequently attains almost steady values. As the area of thermoelectric element increases more thermoelectric material is required which directly affects the cost of the system.

The parallel variations are observed for the thermal efficiency of an irreversible single stage TEG system with area, for different values of T_H in Figure 26. For numerical computation the values of other parameters are chosen as $T_L=300\text{K}$, $K_H=K_L=10\text{W/K}$, $L=0.5\text{mm}$, $I=5\text{A}$ and $N=127$. For a fixed value of T_L as T_H enhances, higher values of thermal efficiency are attained for higher $\Delta T(T_H-T_L)$. The thermal efficiency increases with the area of thermoelectric elements initially whereas, attains almost steady values afterwards. It is recommended to choose the optimum values of area of thermoelectric elements from economical point of view.

Figure 27 and Figure 28 demonstrate the effects of area of thermoelectric couples on output power and thermal efficiency for a predetermined value of T_H and various values of T_L . For numerical computation the values of other parameters are chosen as $T_H=450\text{K}$, $K_H=K_L=10\text{W/K}$, $L=0.5\text{mm}$, $I=5\text{A}$ and $N=127$. As the value of ΔT (T_H-T_L) rises, both power output and thermal efficiency consequently goes up. Hence, the temperature difference source and sink side plays an important in obtaining higher values of performance characteristics of thermoelectric devices. In the beginning, there exists a linear relationship of area of thermoelectric elements and performance parameters, but afterwards power output and efficiency get stabilize.

Figure 29 and Figure 30 exhibit the effects of area of thermoelectric couples on output power and thermal efficiency for different values of external thermal conductance. For numerical computation the values of other parameters are chosen as $T_H=450\text{K}$, $T_L=300\text{K}$, $L=0.5\text{mm}$, $I=5\text{A}$ and $N=127$. The output power increases gradually as external thermal conductance increases.

Figure 31 and Figure 32 demonstrate the effects of area of thermoelectric couples on coefficient of performance (COP) and heating capacity for some predetermined values of T_L and various T_H values. For numerical computation the values of other parameters are chosen as $T_L=250\text{K}$, $K_H=K_L=100\text{W/K}$, $L=0.5\text{mm}$, $I=9\text{A}$ and $N=127$. As the value of ΔT (T_H-T_L) rises, COP of an irreversible single stage TEHP system consequently goes down. With the increase in area, COP initially increases and attains a stable value afterwards. Hence, to design a practical space conditioning system one should judiciously chose the area of thermoelectric elements as area effect the economic aspects of the system. *Figure 32* illustrates the relationship of area and heating capacity for an irreversible single stage TEHP system for a predetermined value of T_L and different values of T_H . The heating capacity possesses inverse relationship with area and ΔT (T_H-T_L).

Figure 33 and Figure 34 exhibit the effects of area of thermoelectric couples on coefficient of performance (COP) and heating capacity for a predetermined T_H value and different T_L values. For numerical computation the values of other parameters are chosen as $T_H=300\text{K}$, $K_H=K_L=100\text{W/K}$, $L=0.5\text{mm}$, $I=9\text{A}$ and $N=127$. As the value of ΔT (T_H-T_L) rises, COP of an irreversible single stage TEHP system subsequently declines. *Figure 34* illustrates the relationship of area and heating capacity for an irreversible single stage TEHP system for a predetermined value of T_H and different values of T_L . The heating capacity possesses inverse relationship with area and ΔT (T_H-T_L).

Figure 35 and Figure 36 exhibit the effects of area of thermoelectric couples on COP and heating capacity for different values of external thermal conductance. For numerical computation the values of other parameters are chosen as $T_H=300\text{K}$, $T_L=250\text{K}$, $L=0.5\text{mm}$, $I=9\text{A}$ and $N=127$. The COP of an irreversible single stage TEHP system declines with rise in external thermal conductances. The heating capacity of the system declines with the rise

in area of thermoelectric couples as shown in Figure 36. Hence, COP and heating capacity attain their maximum values for different values of area of thermoelectric elements and for practical design one has to optimize both simultaneously.

The similar effect has been observed for the length of thermoelectric couples on output power /thermal efficiency for TEG system and COP/heating capacity for TEHP system. The direct relationship of area and length has been shown in Figure 24. It is concluded from above studies that for geometric parameters put considerable effect on the performance parameters as well as economic aspects of designing of thermoelectric devices. Cost of thermoelectric material is concerned with the geometry of thermoelectric elements. For real designing, performance and cost should be optimized simultaneously in order to achieve most effective operation of thermoelectric devices in minimum possible cost.

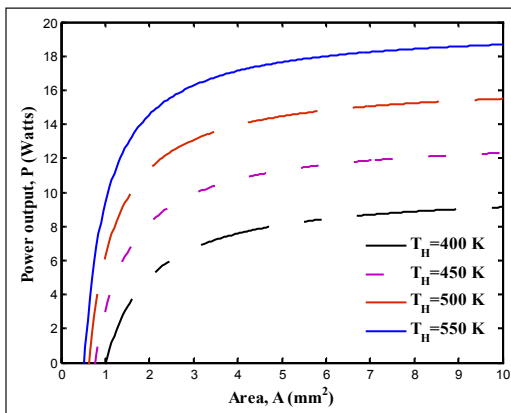


Figure 25. Power output vs area with different values of 'T_H' and fixed value of T_L for TEG

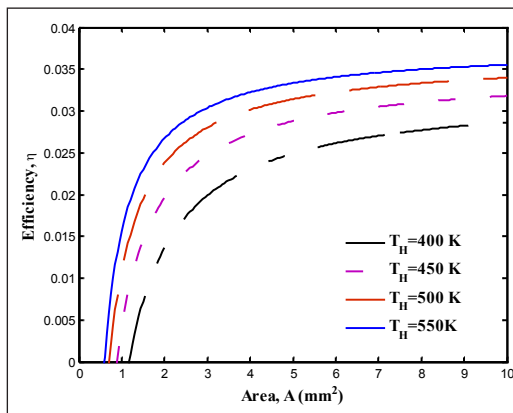


Figure 26. Efficiency vs area with different values of 'T_H' and fixed value of T_L for TEG

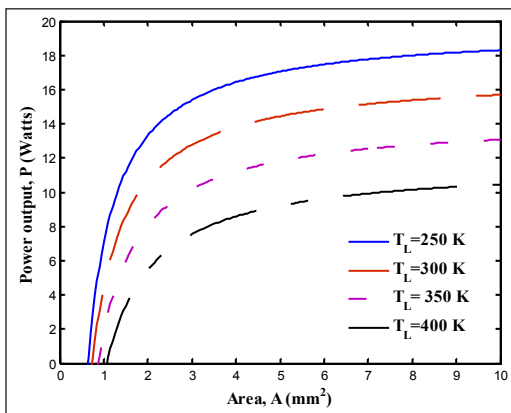


Figure 27. Power output vs area with different values of 'T_L' and fixed value of T_H for TEG

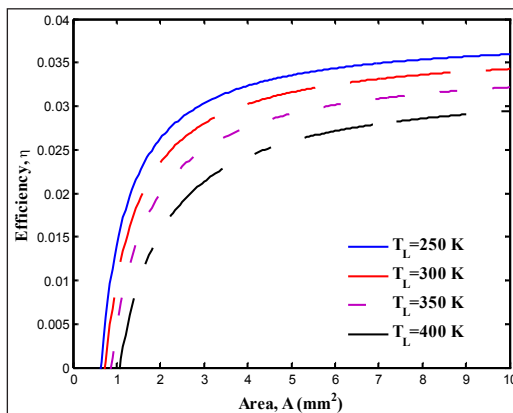


Figure 28. Thermal efficiency vs area with different values of 'T_L' and fixed value of T_H for TEG

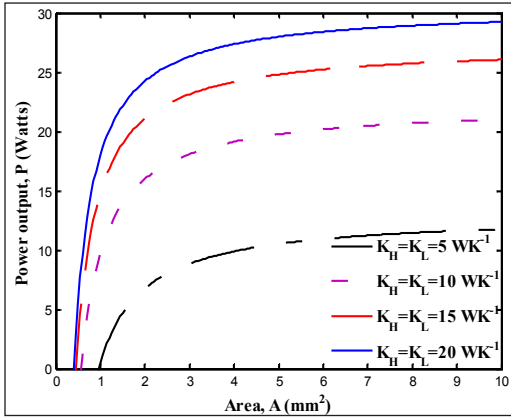


Figure 29. Power output vs area with different values of 'K_H' and 'K_L' for TEG

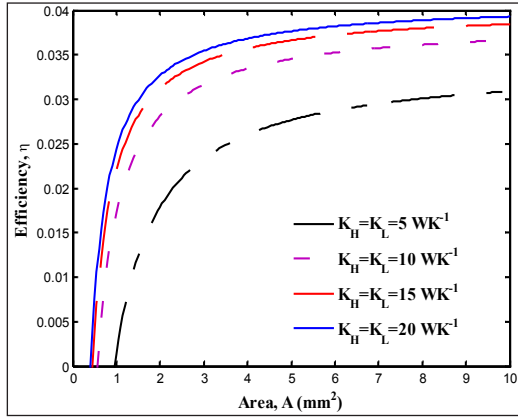


Figure 30. Thermal efficiency vs area with different values of 'K_H' and 'K_L' for TEG

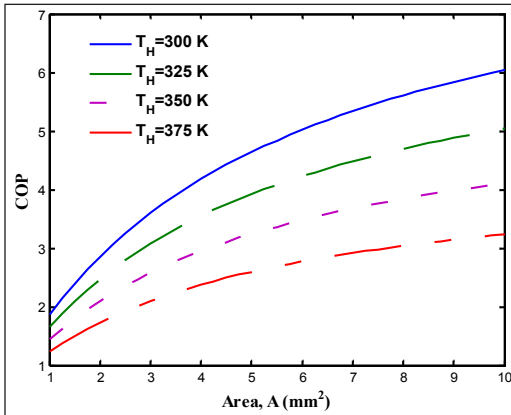


Figure 31. COP vs area with different values of 'T_H' and fixed value of 'T_L' for TEHP

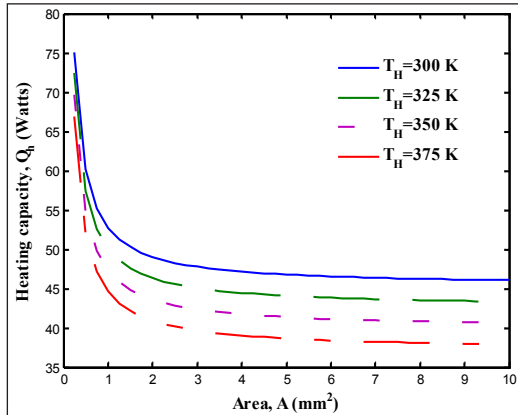


Figure 32. Heating capacity vs area with different values of 'T_H' and fixed value of 'T_L' for TEHP

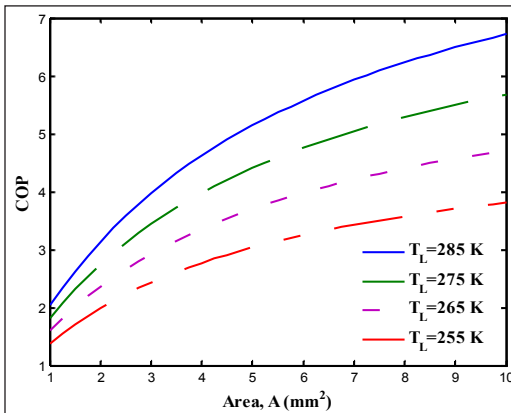


Figure 33. COP vs area with different values of 'T_L' and fixed value of 'T_H' for TEHP

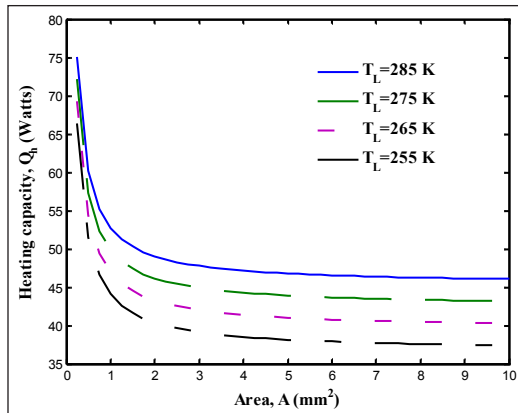


Figure 34. Heating capacity vs area with different values of 'T_L' and fixed value of 'T_H' for TEHP

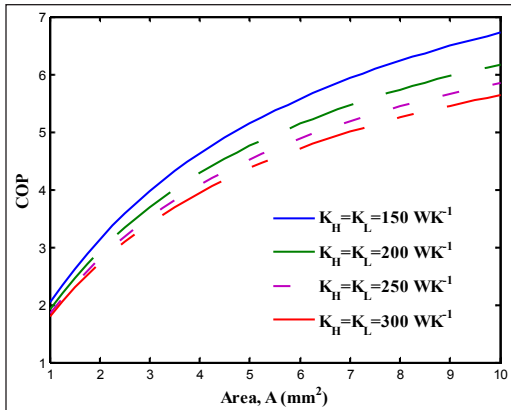


Figure 35. COP vs area with different values of 'K_H' and 'K_L' for TEHP

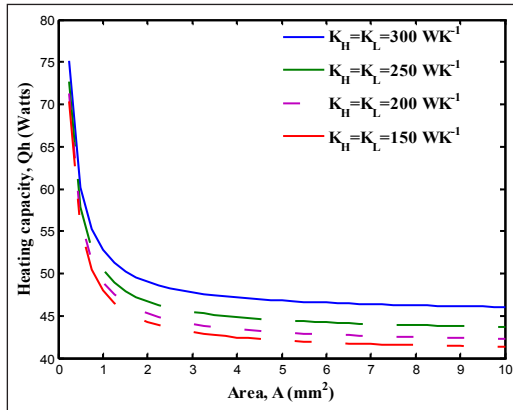


Figure 36. Heating capacity vs area with different values of 'K_H' and 'K_L' for TEHP

Validation of the Study

In order to verify/validate the thermodynamic modeling of TEG and TEHP systems, the data stated in the previous studies are utilized and the comparison is done as illustrated in Table 3. For TEG, the obtained outcomes show an agreement with that of stated in Hogblom and Andersson (2014). Conversely, COP of TEHP obtained in the present work matches with that of stated in Nami et al. (2017) whereas heating capacity matches with that of reported in Kuashik et al. (2015), on the basis of same operating conditions and input parameters.

Table 3
Comparison of designing and performance parameters with previous literature

Comparative Investigations	Designing Parameters								Performance Parameters			
	TEG				TEHP				TEG		TEHP	
	I (A)	T _h (K)	T _c (K)	N	I (A)	T _h (K)	T _c (K)	N	P (W)	η	Q _H (W)	COP
Present Study	2.5	400	300	127	5.12	300	250	127	4.85	0.02	15.12	4.6
Hogblom and Andersson (2014)	4.26	158	65	-	-	-	-	-	5.7	-	-	-
Kaushik et al. (2015)	-	-	-	-	5.65	313	303	-	-	-	14.72	-
Nami et al. (2017)	-	-	-	-	5.6	310	300	-	-	-	-	3.76

CONCLUSION

Finite time thermodynamic analysis carried out on multi-element irreversible TEG and TEHP devices directs the major concluding points as follows:

- The generalized finite time thermodynamic models of TEG and TEHP systems are established considering inner geometrical dimensions, heat transfer in external mode and temperature dependent physical properties.
- Formulation of performance parameters of thermoelectric devices in context with electric current, thermoelectric couples, temperature of hot/cold side and thermal conductances of hot/cold side is presented.
- The analytical formulation of hot/cold sides temperature based on energy balanced equation is achieved for TEG and TEHP devices. The proposed system configurations are investigated with and without heat leak between heat source and sink.
- The effects of design factors on power output/first law efficiency and heating capacity/ coefficient of performance are analyzed.
- The effect of area and length on power output/thermal efficiency, COP and heating capacity is investigated with variations in T_H , T_L , K_H/K_L for single stage TEG and TEHP systems.
- It is concluded from above studies that for geometrical parameters put considerable effect on the performance parameters as well as economic aspects of designing of thermoelectric devices. Cost of thermoelectric material is concerned with the geometry of thermoelectric elements. For real designing, performance and cost should be optimized simultaneously in order to achieve most effective operation of thermoelectric devices.
- It is also observed that various parameters impact the design variables in different ways and performance parameters of thermoelectric devices. The thermodynamic optimization is mandatory and operative for practical operations at variable conditions. The varying features of various input and geometric/design variables obtained in this study is utilized as the benchmark for assessing the effects of external/internal irreversibility on optimum performances of TEG and TEHP systems. Moreover, a practical setup of the proposed thermoelectric systems could be fabricated based on the obtained optimal values of design parameters.

REFERENCES

- Andresen, B. (1983). *Finite-time Thermodynamics*. Physics Laboratory II, University of Copenhagen.
- Angrist, S. W. (1992). *Direct Energy Conversion*. Boston: Allyn and Bacon Inc.
- Chen, J., & Wu, C. (2000). Analysis of the performance of a thermoelectric generator. *Journal of Energy Resource-ASME*, 122(2), 61-63.

- Chen, L., Li, J., Sun, F., & Wu, C. (2005a). Performance optimization of two-stage semiconductor thermoelectric-generator. *Applied Energy*, 82(4), 300-312.
- Chen, L., Li, J., Sun, F., & Wu, C. (2005b). Effect of heat transfer on the performance of two stage semiconductor thermoelectric refrigerators. *Journal of Applied Physics*, 98(3), 1-7. Chen, L., Li, J., Sun, F., & Wu, C. (2008). Performance optimization for a two-stage thermoelectric heat-pump with internal and external irreversibilities. *Applied Energy*, 85(7), 641-49.
- Chen, L., Sun, F., & Chen, W. (1994). Finite time thermodynamic analysis for a thermoelectric refrigerator and heat pump. *Chinese Journal of Engineering Thermophysics*, 15(1), 13–16.
- Chen, W. H., Liao, C. Y., & Hung, C. I. (2012). A numerical study on the performance of miniature thermoelectric cooler affected by Thomson effect. *Applied Energy*, 89(1), 464-473.
- David, B., Ramousse, J., & Luo, L. (2012). Optimization of thermoelectric heat pumps by operating condition management and heat exchanger design. *Energy Conversion and Management*, 60, 125-133.
- Disalvo, F. J. (1999). Thermoelectric cooling and power generation. *Science*, 285(5428), 703- 706.
- Gaurav, K., & Pandey, S. K. (2017). Efficiency calculation of a thermoelectric generator for investigating the applicability of various thermoelectric materials. *Journal of Renewable and Sustainable Energy*, 9(1), 014701.
- Goldsmith, H. J. (1964). *Thermoelectric Refrigeration* (2nd ed.). New York: Wiley.
- Hans, R., Kaushik, S. C., & Manikandan, S. (2016). Performance optimization of two-stage exoreversible thermoelectric heat pump in electrically series, parallel and isolated modes. *International Journal of Energy Technology and Policy*, 12(4), 313-332.
- Hans, R., Manikandan, S., & Kaushik, S. C. (2015). Performance optimization of two-stage exoreversible thermoelectric converter in electrically series and parallel configuration. *Journal of Electronic Materials*, 44(10), 3571-3580.
- Hogblom, O., & Andersson, R. (2014). Analysis of Thermoelectric Generator Performance by Use of Simulations and Experiments. *Journal of Electronic Materials*, 43(6), 2247-2254.
- Kaushik, S. C., Manikandan, S., & Hans, R. (2015). Energy and exergy analyses of thermoelectric heat pump systems. *International Journal of Heat and Mass Transfer*, 86, 843-852.
- Kim, Y. W., Ramousse, J., Fraisse, G., Dalicieux, P., & Baranek, P. (2014). Optimal sizing of a thermoelectric heat pump for heating energy efficient buildings. *Energy Buildings*, 28(70), 106-116.
- Nami, H., Nemati, A., Yari, M., & Ranjbar, F. (2017). A comprehensive thermodynamic and exergoeconomic comparison between single- and two-stage thermoelectric cooler and heater. *Applied Thermal Engineering*, 124, 756-766.
- Riffat, S. B., & Ma, X. (2003). Thermoelectric: a review of present and potential applications. *Applied Thermal Engineering*, 23(8), 913-35.
- Riffat, S. B., & Ma, X. (2004). Improving the coefficient of performance of thermoelectric cooling systems: a review. *International Journal of Energy Research*, 28(9), 753-768.
- Rowe, D. M. (2005). *CRC Handbook of Thermoelectrics*. Boca Raton, Florida: CRC press.

- Sun, X., Liang, X., Shu, G., Tian, H., Wei, H., & Wang, X. (2014). Comparison of the two-stage and traditional single-stage thermoelectric generator in recovering the waste heat of the high temperature exhaust gas of internal combustion engine. *Energy*, 77, 489-498.
- Tan, H., Fu, H., & Yu, J. (2017). Evaluating optimal cooling temperature of single-stage thermoelectric cooler using thermodynamic second law. *Applied Thermal Engineering*, 123, 845-851.
- Xuan, X. C., Ng, K. C., Yap, C., & Chua, H. T. (2002). The maximum temperature differences and polar characteristics of two-stage thermoelectric coolers. *Cryogenics*, 42(5), 273-278.
- Zhu, J., Gao, J., Chen, M., Zhang, J., Du, Q., Rosendahl, L. A., & Suzuki, R. O. (2011). Experimental study of a thermoelectric generation system. *Journal of Electronic Materials*, 40(5), 744-752.